JTTEE5 4:50-58

Influence of Particle Parameters at Impact on Splat Formation and Solidification in Plasma Spraying Processes

M. Vardelle, A. Vardelle, A.C. Leger, P. Fauchais, and D. Gobin

A measurement system consisting of two high-speed two-color pyrometers was used to monitor the flattening degree and cooling rate of zirconia particles on a smooth steel substrate at 75 or 150 °C during plasma spray deposition. This instrument provided data on the deformation behavior and freezing of a particle when it impinged on the surface, in connection with its velocity, size, and molten state at impact. The results emphasized the influence of temperature and surface conditions on particle spreading and cooling. When the substrate temperature was 150 °C, the splats had a perfect lenticular shape, and the thermal interface resistance between the lamella and the substrate ranged from 10^{-7} to 10^{-8} W/m^2 · K. The dependence of the flattening degree on the Reynolds number was investigated.

1. Introduction

THE microstructure and physical properties of a thermally sprayed coating are determined by the dynamics of deformation of the particles impinging on the substrate, the cooling rate of the resulting splats, and the interactions of these splats with the underlying surface. Experimental and theoretical evidence suggests that droplet spreading and cooling on the surface depends on particle size, velocity, and molten state prior to impact and on substrate roughness, temperature, and surface reactivity. However, the number of parameters (often interconnected) involved in the flattening process makes it difficult to fully study and understand these processes.

The objective of this work was to investigate the influence of particle parameters at impact on particle flattening and cooling and to attempt to minimize the dependence on substrate conditions. A measurement system consisting of two high-speed two-color pyrometers was used to monitor particle spreading and freezing as well as particle parameters (size, velocity, and surface temperature) on impact. Results for zirconia particles plasma sprayed onto smooth steel substrates will be presented in terms of flattening time, flattening degree, and cooling rate. The study investigated two substrate temperatures (75 and 150 °C), each of which resulted in a different splat morphology: either distorted shapes at 75 °C or perfect disks at 150 °C. When the substrate was kept at the latter temperature, the investigated conditions were similar to those generally assumed in numerical simulations of droplet impingement in spraying processes. In this case, the experimental results were compared with the values computed from correlations proposed by various investigators (Ref 1-5). Moreover, calculation of splat freezing and cooling was performed using a heat flow model that tracked the solid/liquid interface. This model made it possible to estimate the quenching of the splat from the liquid state down to the substrate temperature, and thus to complete the data from the pyrometric system, which was unable to measure splat temperatures below 2000 K (Ref 6).

Keywords: cooling rate, Madejski relationship, particle diagnostics, splat formation, splat morphology

M. Vardelle, A. Vardelle, A.C. Leger, and **P. Fauchais,** L.M.C.T.S.—Equipe Plasma, Laser, Matériaux, University of Limoges, Science Faculty, 87060 Limoges, France; **D. Gobin,** F.A.S.T., University of Paris, Campus Universitaire, 91405 Orsay, France.

2. Experiments

2.1 *Measurement Technique*

The deformation behavior and the related cooling of a droplet impinging on a substrate was investigated by measuring thermal radiation. The measurement system consisted of a high-speed two-color pyrometer focused onto the substrate to collect the light emitted by the flattening particle. This optical signal was imaged on the entrance slit of a monochromator, and two output signals, filtered at 632.8 and 832.8 nm, were transmitted to two photomultipliers. After amplification, the signals were recorded by a digital oscilloscope. A second identical pyrometer was focused 1.8 mm before the substrate, making it possible to determine particle parameters (size, velocity, and surface temperature) prior to impact and to link these parameters to particle dynamics of deformation and freezing. A coincidence

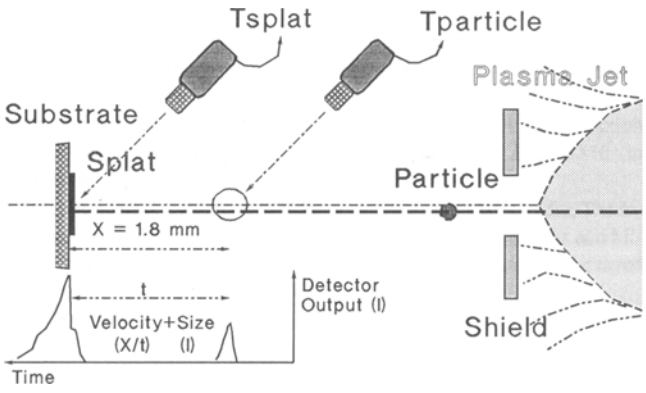

Fig. 1 Schematic of the measurement principle

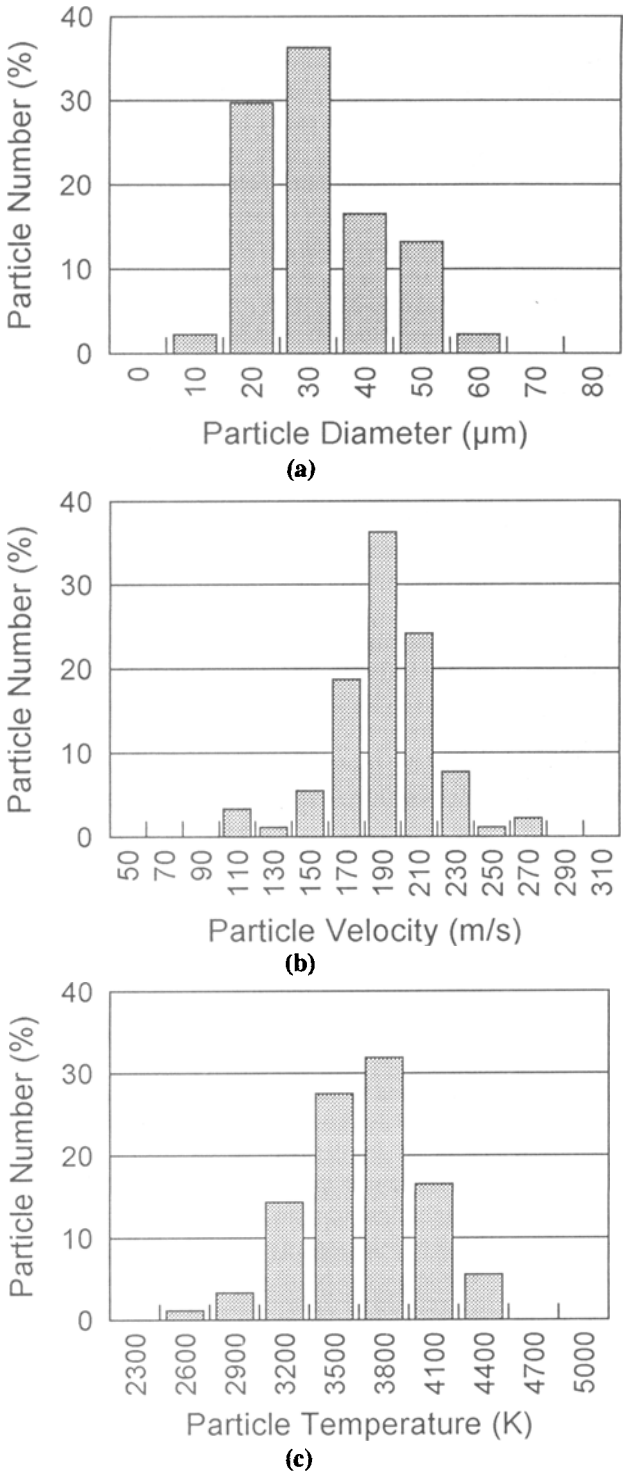

Fig. 2 Distribution of particle size (a), velocity (b), and temperature (c) at an axial location of 120 mm on the torch centerline

sensor focused on the center of the field of view of the second pyrometer ensured that the radiation detected by both pyrometers came from the same particle in flight and at impact.

The spatial resolution for the in-flight measurement was about 0.015 mm^3, and the monitored area on the substrate surface was 0.5 mm^2. The principle of the measurement technique is depicted schematically in Fig. 1 (see Ref 6 for a detailed description of the performance and limitations of the experimental device).

The temperature of the particle or of the splat was derived from the ratio of the photodetector outputs of the pyrometers used for the in-flight or at-impact measurements, respectively, assuming the material behaved as a gray body. Particle velocity was deduced from the time of flight between the focusing points of the two pyrometers. The diameters of the impacting particle and the resulting splat were determined, after calibration, from the maximum of the amplitude of the detector output signals.

When no significant cooling took place during the deformation process, the final flattening time was computed from the rise time of the light signals collected at impact. A mean cooling rate of the splat after the spreading process was complete, was estimated from the time-temperature evolution of the lamella. The cooling rate corresponds to an average computed on about fifteen microseconds or less depending on the shape of the signal emitted during the cooling of the splat. The cooling rate computed in this way only gives an indication of particle cooling just after the completion of the flattening process.

2.2 *Experimental Procedure*

Yttria-stabilized zirconia (8 wt% Y_2O_3) was used in this investigation. Spraying was performed in air using a custom-built torch with a 7 mm diam nozzle. Fused and crushed particles with a nominal diameter of 22 to 45 μm were injected radially 3 mm upstream of the nozzle exit and sprayed onto steel substrates located at 120 mm from the torch nozzle exit. The arc current was 600 A, and the inlet plasma gas flow consisted of a mixture of 45 L/min Ar and 15 L/min H_2.

The experimental method used to study splat formation was based on the presence of a single particle in the measuring volume at every moment. To avoid detecting simultaneous radiation from more than one particle, the powder feed rate was limited to 30 g/h.

The monitored area on the target surface was limited by a 1.5 mm hole positioned 10 mm upstream of the substrate so that only particles following the trajectory close to the plasma jet axis were collected. During experiments, a water-cooled screen with an 8 mm diam hole was located at 20 mm upstream of the second hole. A pneumatic system moved this screen in front of the torch for 1 s. Once 10 particle impacts had been recorded on a substrate, the screen was replaced. This system avoided overlapping of the collected splats, enabling study of particle impingement on a bare substrate.

The target temperature was controlled by an electric resistance heater and monitored by a thermocouple fixed onto its surface. The polished type 304L stainless steel targets had a mean roughness on the order of 0.1 μm. Reference points on the substrate surface allowed location of the impacting particle. Therefore, impact information for a given particle could be linked to the size and morphology of the resulting splat observed by optical microscopy. Splat thickness was measured using either a profilometer with a load of 5.10^{-4} N or an atomic force microscope.

3. Results and Discussion

3.1 *Particle Parameters prior to Impact*

Figures 2(a) to (c) show the measured distributions of particle size, velocity, and temperature, respectively, at the 120 mm axial location on the centerline of the plasma jet. These distributions were determined from a sample of 150 events. The average particle temperature was about 3660 K (almost all the particles had temperatures above the 2950 K melting point of zirconia). The average velocity was 190 m/s, with a standard deviation of 28 m/s. The measured mean particle diameter was 30 μm, which is higher than that estimated by image analysis of the received powder (22 μm). This difference is explained by the detection threshold of the light signal emitted by the in-flight particle, although this threshold was adjusted to a value slightly higher than the background noise.

The Reynolds number calculated using the extreme values of these measured distributions ranged from 350 to 1050, and the corresponding Weber number varied between 3000 and 10,000 (see the appendix to this paper). The former represents the ratio of the inertial force to the viscous force; the latter, the ratio of the inertial force to the surface tension force. The high Weber number values suggest that surface forces are much less significant than viscous forces in determining spreading behavior, as confirmed by different simulations of molten droplet impingement on a substrate (Ref 3, 4).

3.2 *Impacts on Smooth Steel Substrates at Low Temperature (75 °C)*

When zirconia particles are plasma sprayed onto smooth stainless steel substrates kept at low temperature, the resulting splats exhibited distorted shapes with fingerlike perturbations. Moreover, splashing may occur during impact.

The duration of the spreading of the molten material due to impact decreases with particle velocity and temperature, as illustrated in Fig. 3 and 4 for about 100 events. For the range of particle parameters at impact reported in this paper, the flattening time was less than 1.5 μs. The solid lines in these figures, derived by the least-squares approximation technique, show the tendency of flattening time to evolve with the particle parameters prior to impact. The scattering of the experimental data plotted in Fig. 3 and 4 is explained partly by measurement errors (Ref 6) and partly by distributions of the velocity, size, and temperature of particles striking the same point on the substrate surface (Fig. 2a to c). These parameters are not independent and are difficult to control even when using a powder of narrow size distribution.

Smooth surfaces have no excessive roughness to limit droplet spreading. The deformation process is complete when the impact kinetic energy is fully converted into viscous (friction) energy, surface energy, and possible heat flow. As the transient deformation behavior during droplet flattening is monitored from the thermal radiation of its upper surface, no direct information concerning solidification at the fluid flow/substrate interface can be inferred from measurements. However, Bertagnolli et al. (Ref 4) recently investigated the impingement of a zirconia droplet onto a target with a numerical model that included heat transfer and solidification phenomena. Their results show that even when flattening and freezing cannot be treated as separate processes, the influence of solidification on spreading is insignificant. High velocities of the flowing material develop in the upper part of the evolving lamella; thus, the spreading time and the related splat size are nearly the same whether the interaction of heat and fluid flow during flattening is considered or ignored.

Figures 5 and 6 show the flattening degree as a function of particle velocity and temperature, respectively. As expected, this parameter (computed as the ratio of splat diameter to impacting droplet diameter) increases with particle velocity and temperature. An increase in velocity at impact results in an increase in kinetic energy, whereas a rise in temperature corresponds to a decrease in material dynamic viscosity and, thus, in viscous force.

The splat size deduced from the maximum signal intensity detected at impact is always greater than that observed. Only a fraction of the flattened droplet remains on the 75 °C smooth surface after solidification. In this case, the mean splat size determined from the light signal emitted by the particles impacting

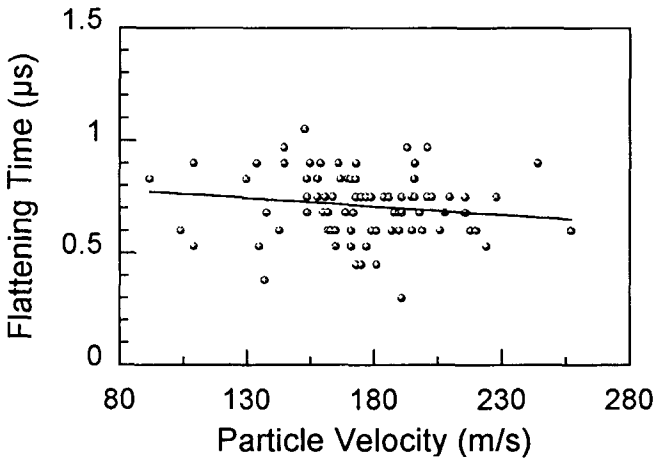

Fig. 3 Flattening time as a function of particle velocity

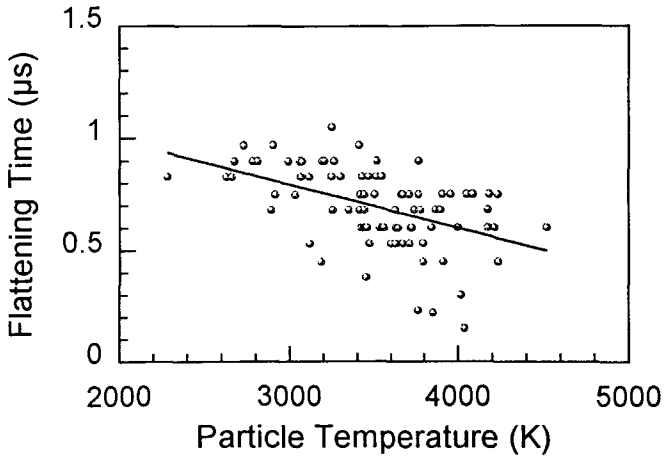

Fig. 4 Flattening time as a function of particle temperature

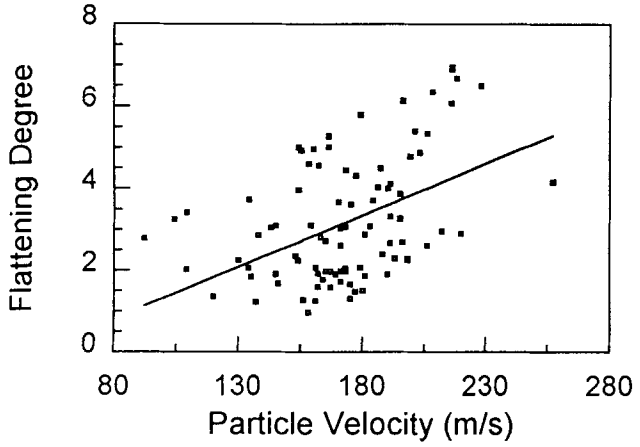

Fig. 5 Flattening degree as a function of particle velocity

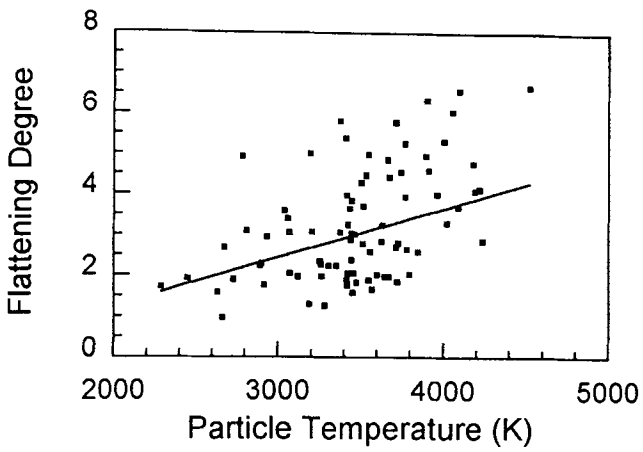

Fig. 6 Flattening degree as a function of particle temperature

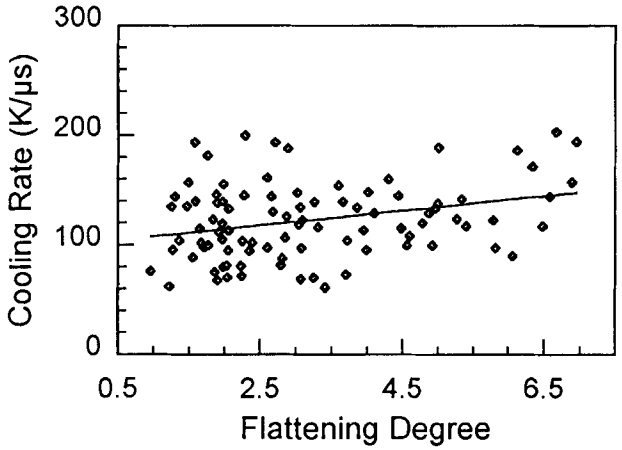

Fig. 7 Cooling rate as a function of flattening degree

on the substrate was approximately 100 μm and the observed average value was about 62 μm. This difference is explained by the loss of a part of the impacting droplet by splashing of the flowing material (which is promoted by droplet velocity and size) and by possible shrinkage of the solidified lamella. The latter mechanism favors the debonding of the nonadhesive portions of the splat. The thickness of the splats that appeared to be attached to the substrate varied over a wide range and was irregular (for a given impact velocity and temperature), but was always between 2 and 4 μm.

The cooling rate of a splat depends on its thickness, the nature of the interface with the underlying surface, and the thermal properties of the materials. When the substrate surface was at 75 °C, the physical contact between the splat and the substrate was limited to small distributed contact points between both (Ref 7), as shown by optical micrographs of the cross sections of plasma spray coatings. The rate of heat removal was then limited by the interface condition. The slight increase in cooling rate with flattening degree, as shown in Fig. 7, is explained by the decrease in splat thickness. For the present conditions, the cooling rate was approximately 100 to 150 K/μs.

3.3 *Impacts on Smooth Steel Substrate at Temperatures Greater than 150 °C*

All the particles flattened on a smooth substrate heated at temperatures greater than 150 °C had an ideal lenticular shape with no noticeable evidence of possible splashing during the deformation process. Moreover, their thickness was regular and their cross sections exhibited a profile with a little thicker rim (Fig. 8a and b). The thickness of the lamellae ranged between 0.5 and 1.5 μm. For particle impact velocities greater than 220 m/s, the splat thickness was between 0.5 and 0.75 μm and the peripheral regions exhibited poor contact with the substrate. This was revealed by observation of the thermogram registered during splat cooling and by observation of a microcrack network at the lamella surface. This network, which originated during relaxation of the quenching stresses, was much more contracted in the central part than in the periphery. The better adhesion of the central part of the thin lamella may be favored by a rapid pressure increase in the droplet at the point of impact.

The high cooling rates (>400 K/μs) achieved under such conditions reflect an intimate contact between the splat and the substrate. However, it should be recalled that the splat cooling rate estimated from the experimental thermograms obtained by pyrometry corresponds to a mean value computed on about 10 to 15 μs just after completion of the flattening process. This value might be lower when computed on the entire splat cooling process, as suggested by the numerical simulation of splat freezing presented in Section 4.

The good contact at the splat/substrate interface favors heterogeneous nucleation with epitaxial growth of columnar crystals through the lamella from the substrate interface. Figure 8(c) shows the surface of a splat and reveals the columnar grain structure, with a column width ranging from 0.05 to 0.1 μm. The intimate bonding at the particle/substrate interface may arise from improved wetting of the hot substrate by the flowing liquid.

The spreading and cooling processes are not quite independent at such cooling rates. Comparison of the size of the splat determined from the maximum amplitude of signal intensity detected at impact and that measured using a profilometer shows an underestimation of the lamella diameter with the former method, attributed to a drop in surface temperature during the

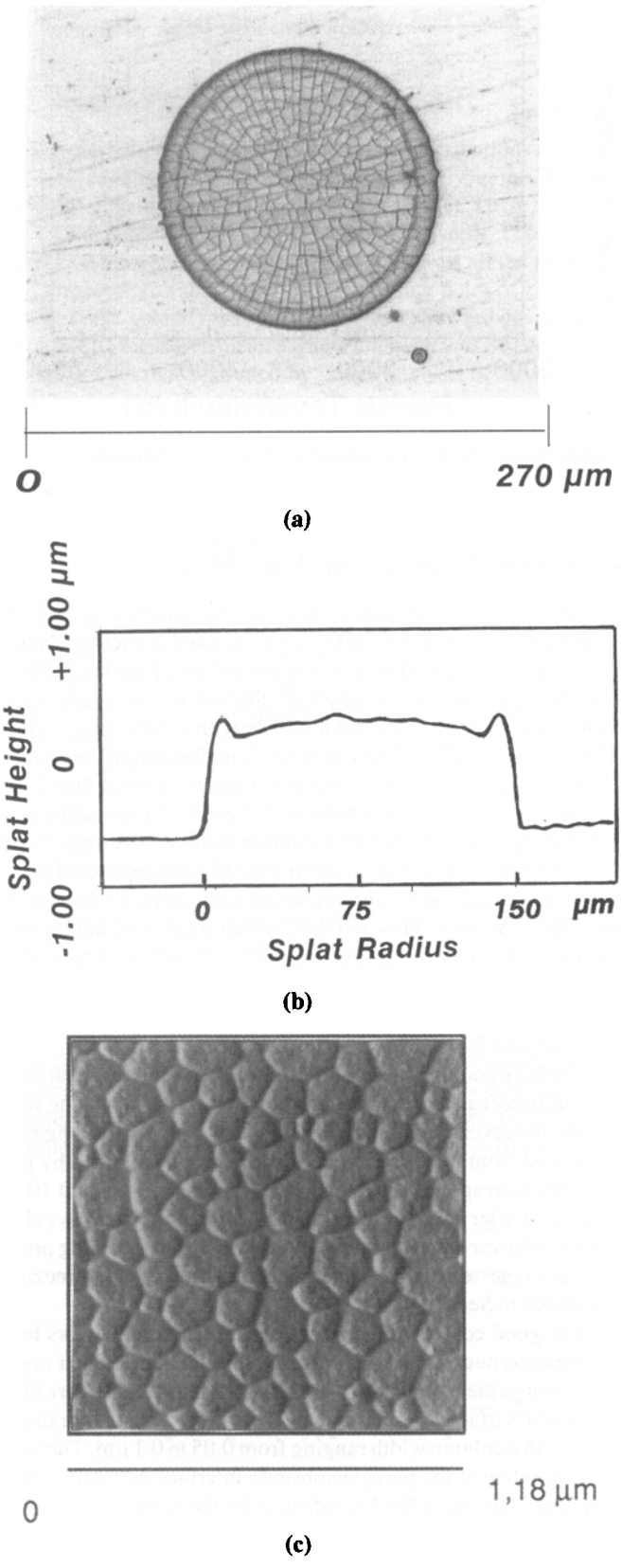

Fig. 8 Zirconia splat on a smooth steel substrate at 150 °C. (a) Electron micrograph. (b) Profile of the thickness of the splat shown in (a). (c) Detail of the surface of the splat shown in (a), revealing the columnar structure

flattening process (Ref 8). This cooling, which is associated with an increase in material viscosity, may promote the perfect disk shape of the splat.

Under the present conditions, the liquid material spreads symmetrically outward from the impact area. This leads to determination of precise values of the diameter and thickness of a given splat (by using a profilometer) in connection with its temperature, velocity, and size prior to impact. Moreover, the diameter of the impacting particle can be computed from the splat dimensions—assuming equal masses of the molten spherical impinging particle and of the resulting cylindrical splat. This allows reduction of the largest source of pyrometer system error, which originates in the measurement of particles and splat sizes and the related calibration (Ref 6).

The evolution of the flattening degree with the Reynolds number computed from the particle parameters measured at impact is given in Fig. 9. An analytical model of the deformation behavior of a molten particle spreading on a surface developed by Madejski (Ref 1) shows that the flattening degree can be computed from $D/d = 1.2941\ \mathrm{Re}^{0.2}$.

More recently, different numerical representations of the time-dependent spreading process have been proposed (Ref 2-5). Regression analysis of these numerical results shows that the dependence of splat size on Reynolds number can be approximated by expressions similar to that calculated by Madejski. These correlations are summarized in Table 1.

The equations established by Madejski (Eq 1) (Ref 1) and Yoshida et al. (Eq 5) (Ref 5), which correspond to the upper and lower values of the flattening degree for a given Reynolds number, are also represented in Fig. 9. The results show reasonable agreement between the experimental values of splat spreading and those predicted by Madejski's correlation. The conditions chosen for the work reported in this section fulfill all the assumptions of Madejski's theory (i.e., smooth substrate, disk-shaped splat, no splashing, perfect interface contact), except for the separation of the flattening and cooling processes. In previous work (Ref 9), where the zirconia particles were plasma sprayed on a substrate at 75 °C, the experimental flattening degrees were consistent with the values computed from the Yoshida et al. equation. The differences between the results of the two studies can be explained by unlike roughnesses and temperatures of the substrate surfaces. On the other hand, the measurements on splats impacting on cool substrates are less accurate and the experimental data more scattered due to the irregular morphologies of the lamellae. This emphasizes the influence of the substrate parameters on the dynamics of splat formation, as confirmed by recent experimental work (Ref 10).

Figure 10 illustrates the dependence of splat cooling rate on Reynolds number. For the reported conditions corresponding to a Reynolds number of less than 1000, an increase in the Reynolds number leads to an increase in the lamella cooling rate. As expected, this freezing speed is a decreasing function of splat thickness (Fig. 11). It should be noted, however, that the cooling rate decreases at about 200 to 500 K/µs for higher Reynolds numbers—that is, for high particle impact velocity—due to the partial debonding of the splat that may occur.

It should be noted also that when the experiments were performed over an extended period of time, lamella morphology changed. The splats exhibited a shape similar to that of splats

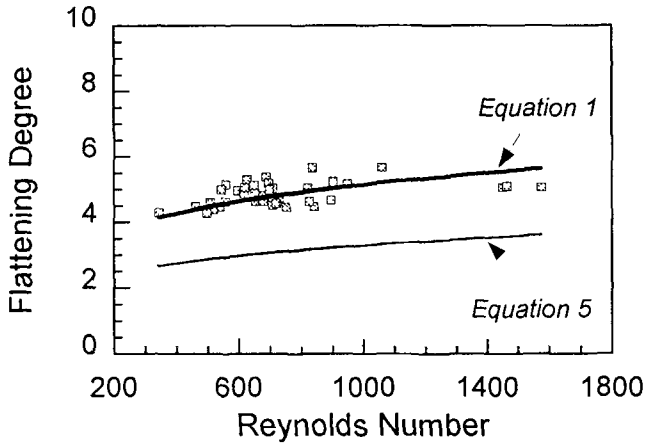

Fig. 9 Flattening degree as a function of Reynolds number. Equations 1 and 5 refer to the data presented in Table 1 for Ref 1 and 5, respectively.

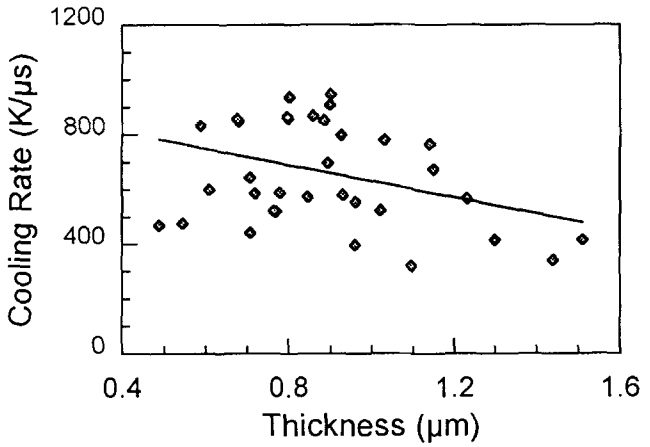

Fig. 11 Splat cooling as a function of splat thickness

sprayed on a low-temperature substrate. The cooling rate in this case is about 100 K/μs. This is attributed to the oxidation of the substrate surface. The thin oxide layer modifies the roughness of the surface and the wetting of the flowing liquid on the substrate (Ref 11).

4. Numerical Simulation of Splat Solidification

4.1 *Physical Model*

When the particles impacted on a substrate held at 150 °C, the resulting splats exhibited a perfect disk shape. In this case, analysis of heat transfer during splat cooling and solidification was performed using a simple mathematical model based on the following three assumptions.

First, the time scale for splat spreading and flattening was assumed to be smaller than the characteristic time for freezing and further cooling of the splat. The purpose of the present model

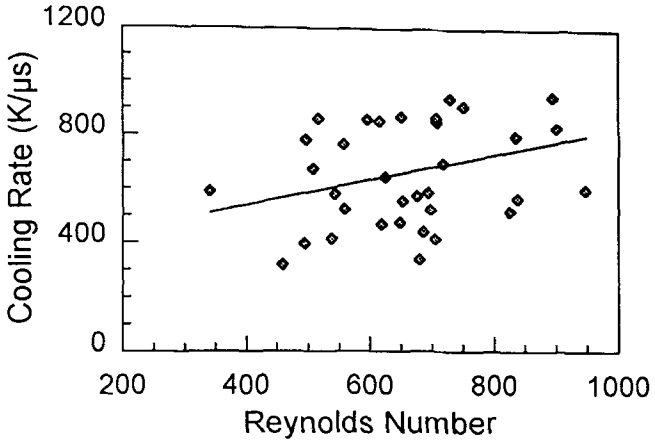

Fig. 10 Dependence of splat cooling on Reynolds number

Table 1 Predicted dependence of flattening degree on Reynolds number ($D/d = a\mathrm{Re}^b$, where $b = 0.2$)

a	Ref
1.2941	1
1	2
1.04	3
0.925	4
0.83	5

was limited to the description of the solidification process. Second, the heat flow in the system was assumed to be essentially in the direction of the impinging particle. The side heat losses could be neglected as shown when using pure conduction simulations with a two-dimensional axisymmetric numerical code. Third, the splat material (zirconia) was considered to be a pure substance solidifying at a given temperature ($T_F = 2950$ K). The phase change mechanism could be described as a pure thermal process, and undercooling was neglected (at this stage of model development).

Taking the above hypotheses into account, a one-dimensional model was developed, consisting of the heat diffusion equation with a moving boundary in the solid and liquid phases, coupled with the heat diffusion equation in the fixed substrate. This phase change problem is a particular configuration in the "Stefan problem," and the phase change condition was written as the energy balance at the interface (Ref 12).

Convective and radiative heat-exchange conditions were assumed at the outer surface of the splat. The quality of the thermal contact between the splat and the substrate was modeled by a thermal resistance. The thermophysical properties of the zirconia/steel system used in calculations are given in the appendix to this paper.

4.2 *Numerical Procedure*

The numerical method used a front immobilization technique based on a classical coordinate transformation first proposed by Landau (Ref 13) and commonly used when front tracking methods involve the solution of phase-change heat transfer problems (Ref 14, 15). The moving physical solid and

liquid domains were thus mapped onto a fixed computational space, and the transformed heat diffusion equations were then explicitly nonlinear, including a pseudoconvective term due to grid deformation in time. The mathematical problem was solved numerically using a well-known finite-volume method (Ref 16).

The implicit formulation of the equations led to an iterative procedure, since the velocity and the position of the solidification front appeared in the coefficients of the transformed equations. An estimate of the front velocity was used to solve the heat diffusion problem in both phases on a time step. The resulting temperature fields were used to solve the energy balance equation at the interface, leading to a new value of the velocity, which was compared with the estimated value. A new cycle was necessary if the relative difference was larger than a prescribed criterion. Numerical runs had been performed to test the accuracy of the method in comparison to the analytical solution of the Stefan problem in a semi-infinite medium.

4.3 *Results and Discussion*

The parameters of the problem were (1) the nature and initial temperature, T_0, of the substrate; (2) the nature, thickness, and initial temperature, T_1, of the splat; and (3) adjustable parameters, such as the convective heat transfer coefficient at the top surface of the splat, or the thermal resistance between the lamella and the substrate.

A first set of simulations showed that the process (splat freezing and subsequent cooling) was dominated by splat thickness and by the initial conditions. The solution was insensitive to heat losses at the particle surface. The relevant outputs of the calculation were the time evolution of the splat surface temperature (which can be compared with the experimental measurements), the time history of the freezing point position, and the temperature profiles in the system at different times.

A typical evolution of the splat surface temperature is shown in Fig. 12, where the corresponding experimental data are also represented (splat thickness = 1.2 μm). The agreement is qualitatively good, and the numerical simulation shows that the order of magnitude of the thermal resistance is very small (about 10^{-8} $W/m^2 \cdot K$). For splats impinging at an impact velocity of less than 220 m/s on a steel substrate at 150 °C, interface thermal resistances range between 10^{-7} and 10^{-8} $W/m^2 \cdot K$. In this case the splat/substrate interface coefficient, h, is quite high. The thermal gradients are then relatively large in both splat and substrate. This situation corresponds practically to ideal cooling (Ref 17).

The interest of the simulation lies in the fact that it reveals a number of details that are not given by the experiment. Figure 12 shows that the surface temperature first decreases very sharply, depending on the initial temperature of the particle. Then, as long as solidification proceeds in the lamella, the temperature remains at a constant level, corresponding to the freezing temperature, T_F. Finally, when the entire splat is in the solid phase, heat extraction of the sensible heat of the particle leads to a very sharp discontinuity in the cooling rate.

The influence of splat thickness and of thermal resistance on cooling rate was investigated, and the results were quantified in terms of the solidification time of the splat and the total cooling time, which was defined as the time necessary for the splat surface temperature to reach 1000 K. In our analysis, T_0 and T_1 were kept constant (300 and 3000 K, respectively), as well as the phase change temperature (T_F = 2950 K).

Figures 13 and 14 show the freezing and cooling times, respectively, versus the thickness of a zirconia splat on a steel substrate for three different interface resistances. When the splat thickness is less than about 1 μm and the contact thermal resistance equal to 10^{-7} or 10^{-8} $W/m^2 \cdot K$, the freezing time is on the order of magnitude of the flattening time. This confirms experimental observations on thin splats collected on a substrate at 150 °C. In this case, it was impossible to determine experimentally the flattening time, as the occurrence of the maximum intensity does not correspond to the termination of the spreading process (Ref 8). This problem arises only for splats of thickness lower than 0.75 μm when the thermal resistance is 10^{-6} $W/m^2 \cdot K$. As Fig. 13 and 14 show, the cooling time is about three times the freezing time. Both cooling and freezing times vary as the square of splat thickness for low thermal resistance ($\leq 10^{-7}$ $W/m^2 \cdot K$), as expected for the ideal cooling situation (Ref 17). For an interface resistance of 10^{-6} $W/m^2 \cdot K$, the cooling ceases to be essentially ideal for lamellae with a thickness of less than about 2 μm.

Figure 15 shows the cooling time of a zirconia splat on a steel or a zirconia substrate. The latter corresponds to the simulation of particles flattened on a previously deposited layer. Both substrate materials have quite different thermal conductivities (about 2 $W/m \cdot K$ for zirconia and 30 $W/m \cdot K$ for steel). Variations in cooling time according to the substrates involved are quite minor for thin splats (<0.5 μm), but become important as lamella thickness increases to 1.5 μm or more. In the case of a 1 μm zirconia splat, the substrate temperature increases up to 1200 K for a steel substrate, whereas it reaches about 2000 K for a zirconia substrate. This appreciable difference lies in the low thermal effusivity of zirconia (about 2800 $J/m^2 \cdot K \cdot s^{0.5}$) compared to that of steel (about 9700 $J/m^2 \cdot K \cdot s^{0.5}$) (see the appendix to this paper for a definition of material effusivity). This low effusivity restrains the diffusion heat released by the cooling of the splat (sensible heat and latent heat of solidification) and thus favors heating of the upper part of the substrate.

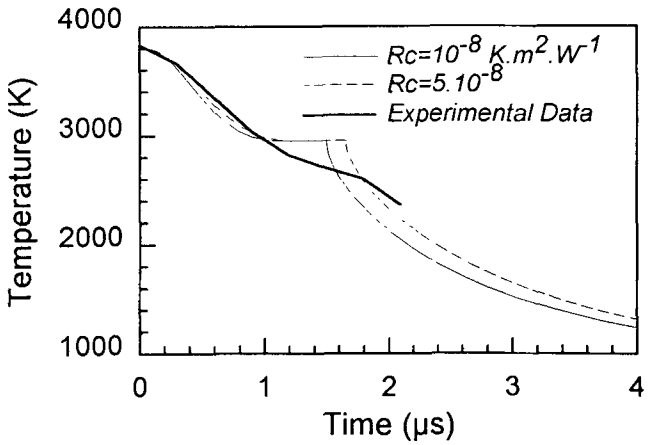

Fig. 12 Experimental and computed thermograms for a 1.2 μm thick zirconia splat in contact with a steel substrate at 150 °C

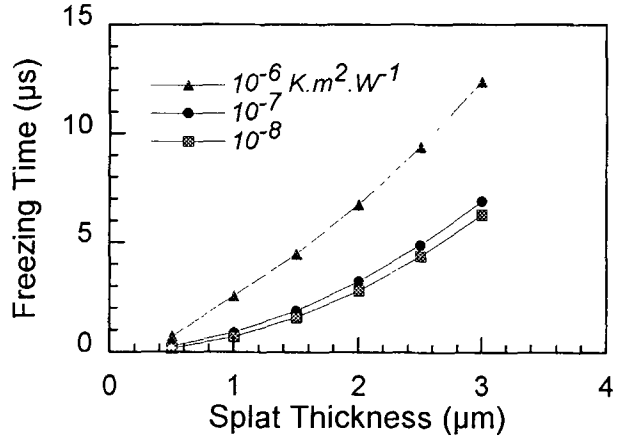

Fig. 13 Splat freezing time as a function of splat thickness at different interface thermal resistances (zirconia splat on a steel substrate at 150 °C)

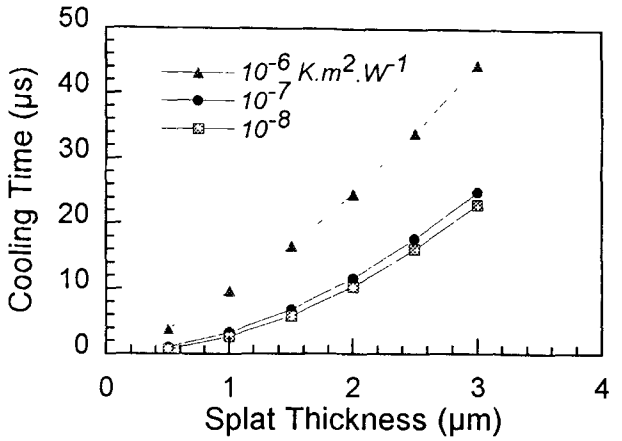

Fig. 14 Splat cooling time as a function of splat thickness at different interface thermal resistance (zirconia splat on a steel substrate at 150 °C)

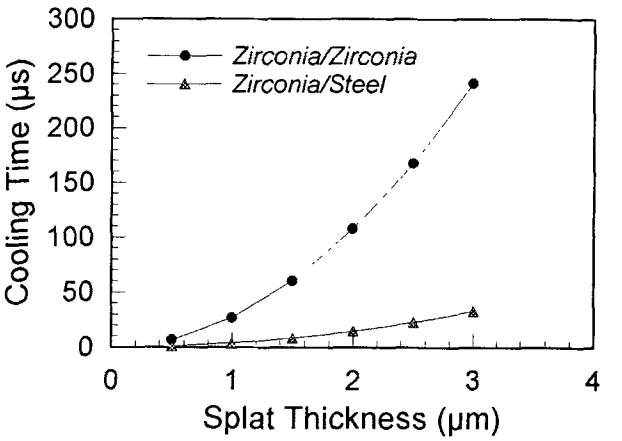

Fig. 15 Splat cooling time as a function of splat thickness for a zirconia splat on a steel or zirconia substrate (interface resistance = 10^{-8} W/m^2 · K)

5. Conclusions

The spreading and cooling of particles plasma sprayed onto flat smooth substrates has been investigated using an experimental device consisting of two high-speed two-color pyrometers. They show the dependence of the flattening and cooling processes on particle velocity, size, and temperature at impact, and also emphasize the influence of substrate roughness, temperature, and oxidation on these processes. When zirconia particles impinge on smooth steel substrates at 150 °C, the intimate contact between the disk-shaped splat and the substrate leads to cooling rate values greater than 400 K/µs. Thus, the spreading and the freezing of the molten droplet are not independent. The interface thermal contact resistance varies between 10^{-7} and 10^{-8} W/m^2 · K. The measured flattening degrees are consistent with those predicted by Madejski's equation (Ref 1). On the other hand, when particles are sprayed on steel substrates at 75 °C or on oxidized hot substrates, the resulting lamellae have distorted morphologies. The real interface contact is restricted to small contact points. The splat cooling rate is about 100 K/µs, which corresponds to an interface thermal resistance greater than 10^{-6} W/m^2 · K.

Cooling rate depends to a great extent on the real contact between the lamellae and the substrate and between the lamellae themselves. Good contact between the lamellae or between the lamellae and the substrate is linked to the cohesion/adhesion of the coating. This has been demonstrated by spraying zirconia on cold ($T < 150$ °C) and hot ($T > 200$ °C) substrates. The cohesion/adhesion more than doubled when hot substrates were used (Ref 18).

Acknowledgment

The experimental work presented in this paper was supported by the Commission of the European Union under the BRITE-EURAM program (BREU/0418).

Appendix

- Re (Reynolds number) = $\rho v d/\mu$ where v is the velocity of the particle at impact, d is particle diameter, and ρ and μ are the density and dynamic viscosity, respectively, of the molten material.
- We (Weber number) = $\rho v^2 d/\sigma$, where σ is surface tension.
- Effusivity = $(\kappa \rho Cp)^{0.5}$, where κ and Cp are the thermal conductivity and the specific heat, respectively, of the material. Effusivity characterizes the heat flux gained or lost by a surface.

References

1. J. Madejski, Solidification of Droplets on a Cold Surface, *Int. J. Heat Mass Transfer*, Vol 19, 1976, p 1009-1013
2. G. Trapaga and J. Szekely, Mathematical Modeling of the Isothermal Impingement of Liquid Droplets in Spraying Processes, *Metall. Trans. B*, Vol 22B, 1991, p 901-914
3. H. Liu, E.J. Lavernia, and R.H. Rangel, Numerical Simulation of Impingement of Molten Ti, Ni, and W Droplets on a Flat Substrate, *J. Thermal Spray Technol.*, Vol 2, 1993, p 369-378
4. M. Bertagnolli, M. Marchese, G. Jacucci, S. Noelting, and I. Doltsinis, "Thermomechanical Simulation of the Splashing Process of a Ceramic

Table 2 Physical data used for calculating Re and We

Property	Value
Zirconia density	5700 kg/m^3
Dynamic viscosity(a)	0.1 exp (–2.95 + 5993/T) kg/m · s
Surface tension	0.5 J/m^2

(a) This equation corresponds to the evolution of alumina viscosity versus temperature.

Table 3 Thermophysical properties of the zirconia/steel system

Property	Zirconia	Steel
Thermal conductivity, W/m · K	2.32	30
Density, kg/m^3	5700	7800
Specific heat, J/kg · K	604	400
Emissivity	1	...
Melting temperature, K	2950	...
Latent heat, J/kg	706,860	...

Droplet on a Rigid Substrate," presented at International Energy Technology Conference (New Orleans), 23-26 Jan 1994

5. T. Yoshida, T. Okada, H. Hamatami, and H. Kumaoka, Integrated Fabrication Process for Solid Oxide Fuel Cells Using Novel Plasma Spraying, *Plasma Sources Sci. Technol.*, Vol 1, 1992, p 195-201
6. M. Vardelle, A. Vardelle, P. Fauchais, and C. Moreau, Pyrometer System for Monitoring the Particle Impact on a Substrate during Plasma Spray Process, *Meas. Sci. Technol.*, Vol 5, 1994, p 205-212
7. R. McPherson, The Relationship between the Mechanism of Formation, Microstructure and Properties of Plasma-Sprayed Coatings, *Thin Solid Films*, Vol 83, 1981, p 297-310
8. C. Moreau, P. Cielo, and M. Lamontagne, Flattening and Solidification of Thermally Sprayed Particles, *J. Therm. Spray Technol.*, Vol 1, 1992, p 317-323
9. S. Fantassi, M. Vardelle, A. Vardelle, and P. Fauchais, Influence of the Velocity of Plasma-Sprayed Particles on Splat Formation, *J. Thermal Spray Technol.*, Vol 2, 1993, p 379-384
10. C. Moreau, M. Lamontagne, and P. Cielo, Influence of the Coating Thickness on the Cooling Rates of Plasma Sprayed Particles Impinging on a Substrate, *Surf. Coat. Technol.*, Vol 53, 1992, p 107-114
11. N. Eustathopoulos and B. Drevet, Mechanisms of Wetting in Reactive Metal/Oxide Systems, *Mater. Res. Soc. Symp. Proc.*, Vol 314, 1993, p 15-26
12. J. Crank, *Free and Moving Boundary Problem*, Oxford University Press, 1984
13. M.G. Landau, Heat Conduction in a Melting Solid, *Q. Appl. Math.*, Vol 8, 1950, p 81-94
14. D. Gobin, "Solid-Liquid Phase Change: Effect of Natural Convection in the Liquid Phase," Thèse d'Etat, University of Paris, 1984 (in French)
15. E.M. Sparrow and W. Chuck, An Implicit/Explicit Numerical Scheme for Phase Change Problems, *Num. Heat Transfer*, Vol 7, 1981, p 1-15
16. S.V. Patankar, *Numerical Heat Transfer and Fluid Flow*, Hemisphere Publishing, 1980
17. R.C. Ruhl, Cooling Rates in Splat Cooling, *Mater. Sci. Eng.*, Vol 1, 1967, p 313-320
18. L. Bianchi, A. Grimaud, F. Blein, and P. Fauchais, Comparison of Plasma Sprayed Ceramic Coatings by RF and DC Plasma Spraying, *Thermal Spray Industrial Applications*, C.C. Berndt and S. Sampath, Ed., ASM International, 1994, p 569-574